# Computation of Limit Loads for Bending Plates

**Trung-Dung Tran**

Faculty of Civil Engineering, Ho Chi Minh City Open University, Vietnam
dung.ttrung@ou.edu.vn

**Phu-Huan Vo Nguyen**

Infrastructural Technique Department, Faculty of Civil Engineering, Ho Chi Minh City Open University, Vietnam
huan.vnp@ou.edu.vn
(corresponding author)

## ABSTRACT

The purpose of this paper is to present a method for calculating the upper bound limit loads of plate bending using a conforming Hsieh-Clough-Tocher (HCT) element. These limit loads can be obtained from Koiter's kinematic shakedown theorem for the case of one load vertex instead of using the kinematic limit theorem. When combining this theorem with the approximated displacement field, the limit analysis turns into an optimization problem and can be effectively solved by Second-Order Cone Programming (SOCP). Several benchmark plate problems such as square, rectangular, and L-shape plates are investigated to illustrate the effectiveness of the proposed solution. The results of the proposed method show good agreement with the results of previous studies. The maximum error is only 2.91% for the fully clamped rectangular plate problem.

*Keywords-plate bending; limit analysis; second-order cone programming; plates; shakedown*

## I. INTRODUCTION

One of the most significant issues in structure engineering is the determination of the safety load factors. Limit analysis is a well-known efficient approach for resolving the issue. These limit loads can be calculated by using the lower- or upper-bound theorems of limit analysis. However, it is very difficult to apply these two theorems to tackle general problems when using analytical methods [1]. Therefore, the current research is mainly concentrated on computational methods. Authors in [2, 3] carried out experimental tests in order to understand the punching shear behavior of concrete slabs reinforced by steel collars and hybrid fibers. Author in [4] studied the limit state of local instability of steel column structures under axial compression using the energy method combined with the finite element method using fiber beam-column elements. Authors in [5] employed the shaft-grouted method to improve the bearing capacity of barrette piles for high-rise buildings in Ho Chi Minh City, Vietnam. Authors in [6] developed a new effective finite element modeling for predicting the ultimate strength of concrete-filled steel tube columns under axial compression. Authors in [7, 8] studied steel frames under static and earthquake loadings with limit load analysis methods. Various discretization techniques have been developed to treat the limit problems such as finite elements [9-12], meshfree methods [13-17], and isogeometric analysis [18].

Limit analysis of plate bending has been extensively investigated, analytically and numerically [19, 20]. In [19], limit loads of plate bending were studied in both Kirchhoff and Mindlin plate models based on the upper bound theorem and the finite element method. A dual algorithm combined with DKQ elements for limit and shakedown analyses of plate bending was proposed in [21]. One of the most efficient methods to conduct plate bending limit analysis was developed by Canh [12, 17], where SOCP was utilized in conjunction with conforming the HCT element or the meshless Element-Free Galerkin (EFG) method. Based on this approach, the aim of this research is to provide a solution to determine the upper bound load factors of plate bending with the combination of the HCT element and SOCP. However, the limit loads will be determined from Koiter's kinematic shakedown theorem for the case of one load vertex instead of using the kinematic theorem of limit analysis as in [12]. The advantage of this approach is that it can be easily extended to the shakedown problem. In addition, having calculated the stress components, it is possible to determine the failure mode of structures such as alternating plasticity for non-shakedown problems [22].

## II. LIMIT ANALYSIS FORMULATION OF PLATE BENDING BASED ON THE SHAKEDOWN APPROACH

Consider a rigid-perfectly plastic plate that has a closed boundary with plane area $A$. Let $\partial A_{\sigma}$ and $\partial A_{\sigma}$ denote static and kinematic boundaries respectively. Neglecting the shear deformation, the kinematic relations of thin plates can be described as:

$$\dot{\boldsymbol{\kappa}} = \begin{bmatrix} \dot{\kappa}_{xx} & \dot{\kappa}_{yy} & 2\dot{\kappa}_{xy} \end{bmatrix} = \nabla^2 \dot{\omega} \qquad (1)$$

where $\dot{\boldsymbol{\kappa}}$ denotes the curvature rate vector, $\dot{\omega}$ is the transversal velocity, and the operator $\nabla^2$ is expressed by:

$$\nabla^2 = \begin{bmatrix} \dfrac{\partial^2}{\partial x^2} & \dfrac{\partial^2}{\partial y^2} & 2\dfrac{\partial^2}{\partial x \partial y} \end{bmatrix}^T$$

Let $\mathbf{m} = \begin{bmatrix} m_{xx} & m_{yy} & 2m_{xy} \end{bmatrix}^T$ and $p$ be the vector of bending moments and the transversal load, respectively. The equilibrium relation can be defined as:

$$\left( \nabla^2 \right)^T \mathbf{m} - p = 0 \qquad (2)$$

In this study, the von Mises yield condition is adopted, and the internal dissipation power of the plate bending (or the dissipation rate) can be described as:

$$D^p \left( \dot{\boldsymbol{\kappa}} \right) = m_p \sqrt{\dot{\boldsymbol{\kappa}}^T \mathbf{Q} \dot{\boldsymbol{\kappa}}} \qquad (3)$$

where:

$$\mathbf{Q} = \frac{1}{3} \begin{bmatrix} 4 & 2 & 0 \\ 2 & 4 & 0 \\ 0 & 0 & 1 \end{bmatrix} \qquad (4)$$

and $m_p = \sigma_y h^2 / 4$ is the plastic limit moment per unit length of a plate section in which $h$ and $\sigma_y$ denote the plate thickness and the yield stress, respectively.

Next, consider a structure simultaneously submitted to *NL* linearly independently varying loads $\hat{P}_k = (k = 1, 2, ..., NL)$ which form a convex polyhedral load domain. According to Koiter's theorem [23], by applying mathematical programming theory, an upper bound of the shakedown load factor $\alpha^+$ can be rewritten in the form of non-linear programming as follows (the superscript $p$ of dissipation rate function is skipped for simplicity):

$$\alpha^+ = \min \sum_{k=1}^{NL} \int_A D\left( \dot{\boldsymbol{\kappa}}_k \right) dA$$

$$s.t \begin{cases} \Delta\boldsymbol{\kappa} = \displaystyle\sum_{k=1}^{NL} \dot{\boldsymbol{\kappa}}_k = \nabla^2 \dot{\omega} \\ \dot{\omega} = 0 \qquad on \ \partial A_u \\ \displaystyle\sum_{k=1}^{NL} \int_A \mathbf{m}^e \left( x, \hat{P}_k \right)^T \dot{\boldsymbol{\kappa}}_k dA = 1, \end{cases} \qquad (5)$$

where $\mathbf{m}^e$ is the fictitious elastic moment vector of the point $x$ on the domain A.

Note that, when *NL* = 1 the problem (5) reduces that of limit analysis. Then, the formulation for the upper bound limit load is determined as follows:

$$\alpha^+ = \min \int_A D^P \left( \dot{\boldsymbol{\kappa}} \right) dA$$

$$s.t \begin{cases} \dot{\boldsymbol{\kappa}} = \nabla^2 \dot{\omega} \\ \dot{\omega} = 0 \qquad on \ \partial A_u \\ \displaystyle\int_A \mathbf{m}^{eT} \dot{\boldsymbol{\kappa}} dA = 1, \end{cases} \qquad (6)$$

Compared to the kinematic theorem of limit analysis as presented in [12], the difference of (6) is that the work rate of the applied load constraint is replaced by the external work rate constraint. In general, problem (6) is complicated because it has to calculate the stress components. However, as mentioned above, it can be advantageous to develop the shakedown problem. In addition, the failure mode of alternating plasticity can be determined easily when the structure is subjected to repeated loads.

## III.   HCT-BASED KINEMATIC FORMULATION

The conforming HCT element has been detailed in [12, 24]. The key idea of the HCT element is to divide an original triangular element into three sub-elements as shown in Figure 1.
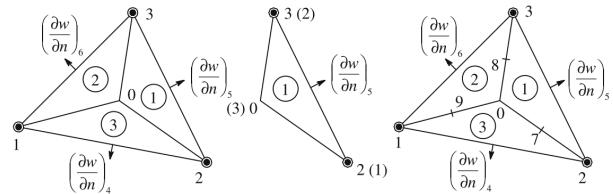


Fig. 1.     HCT element.

The number of the total degrees of freedom of the element is 12 including 3 degrees at each corner node and 3 degrees at three mid-side nodes. In terms of area coordinates $\zeta = (\zeta_1, \zeta_2, \zeta_3)$, at each sub-triangle, we can express the displacement expansion $w^{(k)}$ as follows:

$$w^{(k)} (\zeta) = \left( \mathbf{L}_e^{(k)} (\zeta) + \mathbf{L}_0^{(k)} (\zeta) \mathbf{F} \right) \mathbf{q}_e, \ k = 1, 2, 3 \qquad (7)$$

where $\mathbf{q}_e$ is the element displacement matrix ανδ the partitions $\mathbf{L}_e^{(k)} (\zeta)$ and $\mathbf{L}_0^{(k)} (\zeta)$ denote the interpolation functions, respectively. $\mathbf{F}$ is the matrix determined from compatible conditions. Then, the curvatures can be defined by:

$$\boldsymbol{\kappa}^{(k)} = \begin{bmatrix} \kappa_{xx}^{(k)} \\ \kappa_{yy}^{(k)} \\ \kappa_{xy}^{(k)} \end{bmatrix} = \begin{bmatrix} \mathbf{L}_{e,xx}^{(k)} + \mathbf{L}_{0,xx}^{(k)} \mathbf{F} \\ \mathbf{L}_{e,yy}^{(k)} + \mathbf{L}_{0,yy}^{(k)} ) \mathbf{F} \\ \mathbf{L}_{e,xy}^{(k)} + \mathbf{L}_{0,xy}^{(k)} \mathbf{F} \end{bmatrix} \mathbf{q}_e = \begin{bmatrix} \mathbf{B}_{e,xx}^{(k)} \\ \mathbf{B}_{e,yy}^{(k)} \\ \mathbf{B}_{e,xy}^{(k)} \end{bmatrix} \mathbf{q}_e \qquad (8)$$

and we can obtain the plastic dissipation of the plate as:

$$D = m_p \sum^{ne} \sum^3 \sum^{NG}_{j=1} \xi_j \sqrt{\dot{\boldsymbol{\kappa}}^T(\zeta_j) \mathbf{Q} \dot{\boldsymbol{\kappa}}(\zeta_j)} \qquad (9)$$

where *ne* and *NG* are the total number of elements and Gaussian points, respectively.

The upper-bound limit analysis based on the shakedown approach of plate bending is now described as:

$$\alpha^+ = \min \ m_p \sum^{ne} \sum^3 \sum^{NG}_{j=1} \xi_j \sqrt{\dot{\boldsymbol{\kappa}}^T(\zeta_j) \mathbf{Q} \dot{\boldsymbol{\kappa}}(\zeta_j)}$$

$$s.t \begin{cases} \dot{\boldsymbol{\kappa}}(\zeta_j) = \mathbf{B}_j \dot{\mathbf{q}} \\ \sum^{ne} \sum^3 \sum^{NG}_{j=1} \xi_i \mathbf{m}^e_j \dot{\boldsymbol{\kappa}}^T(\zeta_j) = 1 \\ \dot{\mathbf{q}} = 0 \qquad on \ \partial A_u \end{cases} \qquad (10)$$

By formulating the objective function to a form comprising a sum of norms, the optimization problem (10) can be re-expressed as a standard SOCP as follows [25]:

$$D = m_p \sum^{ne} \sum^3 \sum^{NG}_{j=1} \xi_j \left\| \mathbf{J}^T \dot{\boldsymbol{\kappa}}(\zeta_j) \right\| \qquad (11)$$

where **J** is defined as:

$$\mathbf{J} = \frac{1}{\sqrt{3}} \begin{bmatrix} 2 & 0 & 0 \\ 1 & \sqrt{3} & 0 \\ 0 & 0 & 1 \end{bmatrix} \qquad (12)$$

It can be seen that **J** is also the Cholesky factor of **Q**. Finally, by establishing supplementary variables $x_1$, $x_2$,…, $x_{ne \times 3 \times NG}$, problem (10) can be stated as follows:

$$\alpha^+ = \min \ m_p \sum^{ne \times 3 \times NG}_{k=1} \xi_k x_k$$

$$s.t \begin{cases} \sum^{ne} \sum^3 \sum^{NG}_{j=1} \xi_j \mathbf{m}^e_j \dot{\boldsymbol{\kappa}}^T(\zeta_j) = 1 \\ \dot{\mathbf{q}} = 0 \qquad on \ \partial A \\ \boldsymbol{\rho}_k = \mathbf{J}^T \dot{\boldsymbol{\kappa}}(\zeta_k) \\ \|\boldsymbol{\rho}_k\| \le x_k, \ k = 1, 2, ..., ne \times 3 \times NG \end{cases} \qquad (13)$$

where $\|\boldsymbol{\rho}_k\| \le x_k$ denotes quadratic cones and the $\boldsymbol{\rho}_k$ are supplementary variables.

## IV. NUMERICAL EXAMPLES

To illustrate the effectiveness of the proposed solution, in this section we investigate various benchmark problems that have numerical or analytical solutions. The following parameters are adopted for all examples: length *a* = 10m and plate thickness *h* = 0.1m. The first example considers a square plate with side length *a*, and restraints on all edges that are

either simply supports or clamped. The plate is subjected to uniform pressure *p*, as shown in Figure 2. Due to symmetry, we only modeled the upper-right quarter of the plate as illustrated in Figure 3. The results of the proposed method, normalized with $m_p/a^2$, are presented in Table I. It can be observed that when the number of the elements increases, the collapse load factors reduce and converge. When compared with previous results, the present results are in good agreement with those obtained numerically in [18, 19, 21], in which the EFG method, a $C_1$ continuity plate element, and the the DKQ element were used, respectively. In addition, Table I also shows that the results of the proposed method are similar to the results obtained analytically in [20, 26]. The yield patterns in terms of plastic dissipation distribution are plotted in Figure 4. It can be seen that they are very consistent with the experiment, for both simply supported and clamped plates.
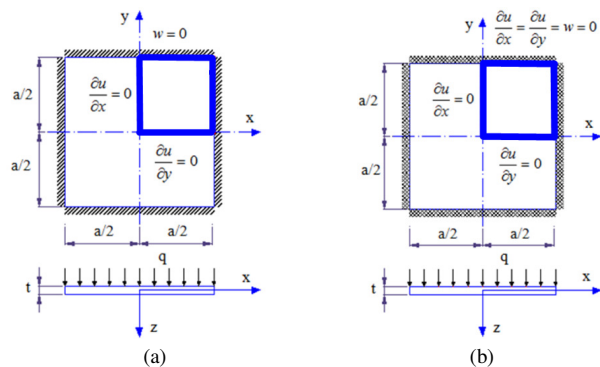


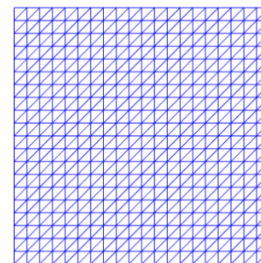Fig. 2.     Square slabs: geometry and loading. (a) Simply supported plate, (b) clamped plate.



Fig. 3.     Square slab: finite element mesh.

TABLE I.     LIMIT LOAD FACTOR OF THE SQUARE PLATE ($pa^2/m_p$)

| Method | | Simply supported | | Clamped | |
|---|---|---|---|---|---|
| | | UB | LB | UB | LB |
| **Proposed** | $N_e = 50$ | 25.18 | - | 51.83 | - |
| | $N_e = 200$ | 25.06 | - | 48.17 | - |
| | $N_e = 800$ | 25.03 | - | 46.19 | - |
| | $N_e = 1800$ | 25.03 | - | 45.58 | - |
| [19] | | 25.02 | - | 45.29 | - |
| [17] | | 25.01 | - | 45.07 | - |
| [21] | | 25.04 | 25.04 | 45.06 | 45.06 |
| [20] | | 26.54 | 24.86 | 49.25 | 42.86 |
| [26] | | 27.71 | 23.81 | 52.01 | - |

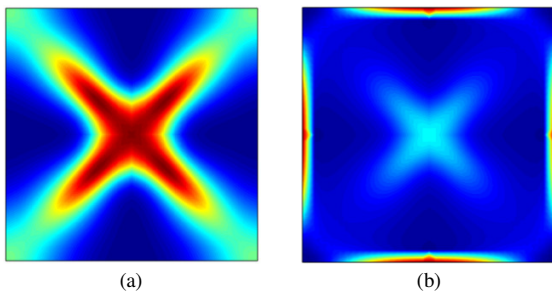$N_e$: number of elements, LB – Lower bound, UB – Upper bound

Fig. 4.     Square slabs: plastic dissipation distribution. (a) Simply supported plate, (b) clamped plate.
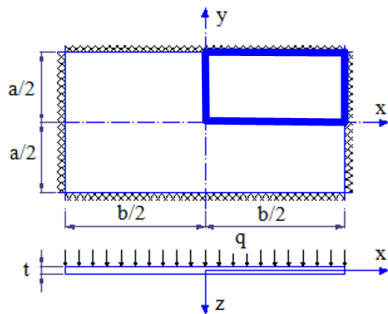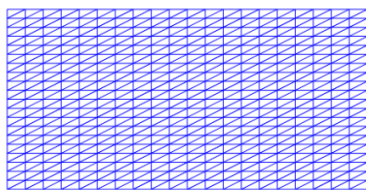


Fig. 5.     Rectangular slab: geometry and loading.



Fig. 6.     Rectangular slab: finite element mesh.

TABLE II.          LIMIT LOAD FACTOR OF THE RECTANGULAR PLATE ($pab/m_p$)

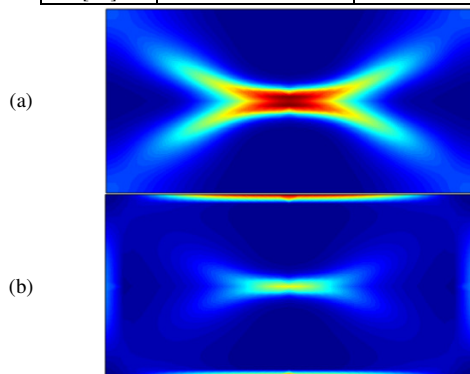| Method | Simply supported | Clamped |
|---|---|---|
| Proposed | 29.90 | 56.20 |
| [19] | 29.88 | - |
| [17] | 29.88 | 54.61 |



Fig. 7.     Rectangular slabs: plastic dissipation distribution. (a) Simply supported plate, (b) clamped plate.

Next, we consider the rectangular slab of Figure 5 (dimensions a×b and b/a = 2). Similar to the previous example, only the upper-right quarter of the plate is modeled by 800

elements (Figure 6). Limit load factors are reported in Table II. When compared with the previously obtained results, the proposed method provides better solutions than in [17, 19] by 0.07% and 2.91% for the case of simply supported and clamped edges, respectively. The plastic dissipation distribution of rectangular slabs is plotted in Figure 7.

The last example is an L-shape plate, investigated in the case of uniform load. The geometry and uniform mesh of the L-shape plate are shown in Figure 8 and the limit load factors are shown in Table III. Again, the results of the proposed method show good agreement with previous studies. The maximum error is only 2.59% for the case of clamped edges. The plastic dissipation distribution using 2400 elements is plotted in Figure 9.
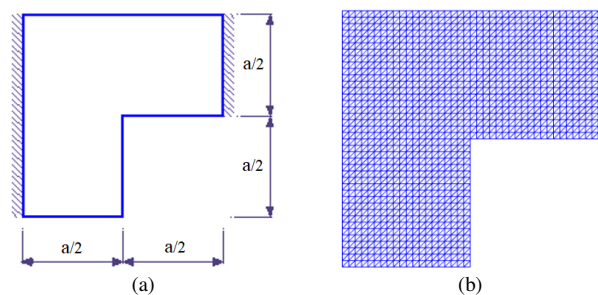


Fig. 8.     L-shape plate. (a) Geometry, (b) Mesh.

TABLE III.          LIMIT LOAD FACTOR OF THE L-SHAPE PLATE ($pa^2/m_p$)

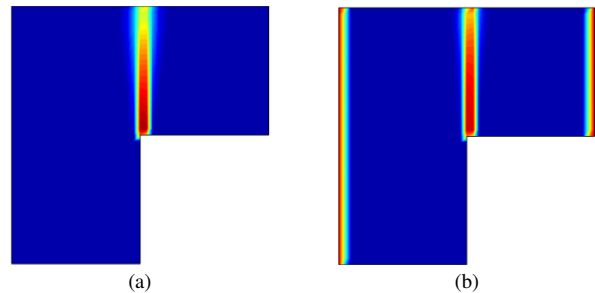| Method | Simply supported | Clamped |
|---|---|---|
| Proposed | 6.20 | 16.24 |
| [10] | 6.29 | - |
| [15] | 6.17/6.04 | 15.83/15.69 |



Fig. 9.     L-shape slabs: Plastic dissipation distribution. (a) Simply supported, (b) clamped.

## V.   CONCLUSION

This paper presented a numerical solution for the computation of the limit loads of bending plates. Using von Mises yield criterion and the conforming HCT element, the upper bound limit load can be derived from Koiter's kinematic shakedown theorem for the case of one load vertex instead of using the upper bound theorem of limit analysis. Based on this approach, the work rate of the applied load constraint in the kinematic theorem of limit analysis is replaced by the external work rate constraint. The formulation based on Koiter's kinematic shakedown theorem is more complicated than the

formulations for the upper bound of the limit load, however, it can be developed to the shakedown problem and the failure mode of alternating plasticity can be determined easily. One benefit of this research is that the problems can be formulated as SOCP, so that they can be solved rapidly, even when many variables are involved. The accuracy and reliability of the proposed solution method were proven by numerical examples.

## ACKNOWLEDGMENT

## REFERENCES

[1] W. Prager and P. G. Hodge Jr., *Theory of Perfectly Plastic Solids*, 1st ed. New York, NY, USA: John Wiley & Sons, 1951.

[2] A. A. Abdulhussein and M. H. Al-Sherrawi, "Experimental and Numerical Analysis of the Punching Shear Resistance Strengthening of Concrete Flat Plates by Steel Collars," *Engineering, Technology & Applied Science Research*, vol. 11, no. 6, pp. 7853–7860, Dec. 2021, https://doi.org/10.48084/etasr.4497.

[3] A. N. Dalaf and S. D. Mohammed, "The Impact of Hybrid Fibers on Punching Shear Strength of Concrete Flat Plates Exposed to Fire," *Engineering, Technology & Applied Science Research*, vol. 11, no. 4, pp. 7452–7457, Aug. 2021, https://doi.org/10.48084/etasr.4314.

[4] P. C. Nguyen, "Local Instability Analysis for Axial Compressive Steel Columns," *Engineering, Technology & Applied Science Research*, vol. 12, no. 6, pp. 9527–9531, Dec. 2022, https://doi.org/10.48084/etasr.5238.

[5] P. H. V. Nguyen and P. C. Nguyen, "Effects of Shaft Grouting on the Bearing Behavior of Barrette Piles: A Case Study in Ho Chi Minh City," *Engineering, Technology & Applied Science Research*, vol. 11, no. 5, pp. 7653–7657, Oct. 2021, https://doi.org/10.48084/etasr.4389.

[6] P. C. Nguyen, D. D. Pham, T. T. Tran, and T. Nghia-Nguyen, "Modified Numerical Modeling of Axially Loaded Concrete-Filled Steel Circular-Tube Columns," *Engineering, Technology & Applied Science Research*, vol. 11, no. 3, pp. 7094–7099, Jun. 2021, https://doi.org/10.48084/etasr.4157.

[7] P. C. Nguyen, B. Le-Van, and S. D. T. V. Thanh, "Nonlinear Inelastic Analysis of 2D Steel Frames : An Improvement of the Plastic Hinge Method," *Engineering, Technology & Applied Science Research*, vol. 10, no. 4, pp. 5974–5978, Aug. 2020, https://doi.org/10.48084/etasr.3600.

[8] P. C. Nguyen, "Nonlinear Inelastic Earthquake Analysis of 2D Steel Frames," *Engineering, Technology & Applied Science Research*, vol. 10, no. 6, pp. 6393–6398, Dec. 2020, https://doi.org/10.48084/etasr.3855.

[9] F. Tin-Loi and N. S. Ngo, "Performance of the p-version finite element method for limit analysis," *International Journal of Mechanical Sciences*, vol. 45, no. 6, pp. 1149–1166, Jun. 2003, https://doi.org/10.1016/j.ijmecsci.2003.08.004.

[10] T. N. Trần, R. Kreißig, and M. Staat, "Probabilistic limit and shakedown analysis of thin plates and shells," *Structural Safety*, vol. 31, no. 1, pp. 1–18, Jan. 2009, https://doi.org/10.1016/j.strusafe.2007.10.003.

[11] D. K. Vu, A. M. Yan, and H. Nguyen-Dang, "A primal–dual algorithm for shakedown analysis of structures," *Computer Methods in Applied Mechanics and Engineering*, vol. 193, no. 42, pp. 4663–4674, Oct. 2004, https://doi.org/10.1016/j.cma.2004.03.011.

[12] C. V. Le, H. Nguyen-Xuan, and H. Nguyen-Dang, "Upper and lower bound limit analysis of plates using FEM and second-order cone programming," *Computers & Structures*, vol. 88, no. 1, pp. 65–73, Jan. 2010, https://doi.org/10.1016/j.compstruc.2009.08.011.

[13] S. Chen, Y. Liu, and Z. Cen, "Lower-bound limit analysis by using the EFG method and non-linear programming," *International Journal for Numerical Methods in Engineering*, vol. 74, no. 3, pp. 391–415, 2008, https://doi.org/10.1002/nme.2177.

[14] P. L. H. Ho and C. V. Le, "A stabilized iRBF mesh-free method for quasi-lower bound shakedown analysis of structures," *Computers &*

*Structures*, vol. 228, Feb. 2020, Art. no. 106157, https://doi.org/10.1016/j.compstruc.2019.106157.

[15] P. L. H. Ho, C. V. Le, and T. Tran-Cong, "Limit state analysis of reinforced concrete slabs using an integrated radial basis function based mesh-free method," *Applied Mathematical Modelling*, vol. 53, pp. 1–11, Jan. 2018, https://doi.org/10.1016/j.apm.2017.08.006.

[16] C. V. Le, H. Askes, and M. Gilbert, "Adaptive element-free Galerkin method applied to the limit analysis of plates," *Computer Methods in Applied Mechanics and Engineering*, vol. 199, no. 37, pp. 2487–2496, Aug. 2010, https://doi.org/10.1016/j.cma.2010.04.004.

[17] C. V. Le, M. Gilbert, and H. Askes, "Limit analysis of plates using the EFG method and second-order cone programming," *International Journal for Numerical Methods in Engineering*, vol. 78, no. 13, pp. 1532–1552, 2009, https://doi.org/10.1002/nme.2535.

[18] H. V. Do and H. Nguyen-Xuan, "Limit and shakedown isogeometric analysis of structures based on Bézier extraction," *European Journal of Mechanics - A/Solids*, vol. 63, pp. 149–164, May 2017, https://doi.org/10.1016/j.euromechsol.2017.01.004.

[19] A. Capsoni and L. Corradi, "Limit Analysis of Plates-a Finite Element Formulation," *Structural Engineering and Mechanics: An International Journal*, vol. 8, no. 4, pp. 325–341, Oct. 1999, https://doi.org/10.12989/sem.1999.8.4.325.

[20] P. G. Hodge Jr. and T. Belytschko, "Numerical Methods for the Limit Analysis of Plates," *Journal of Applied Mechanics*, vol. 35, no. 4, pp. 796–802, Dec. 1968, https://doi.org/10.1115/1.3601308.

[21] T. N. Tran, "A dual algorithm for shakedown analysis of plate bending," *International Journal for Numerical Methods in Engineering*, vol. 86, no. 7, pp. 862–875, 2011, https://doi.org/10.1002/nme.3081.

[22] T. D. Tran, C. V. Le, D. C. Pham, and H. Nguyen-Xuan, "Shakedown reduced kinematic formulation, separated collapse modes, and numerical implementation," *International Journal of Solids and Structures*, vol. 51, no. 15, pp. 2893–2899, Aug. 2014, https://doi.org/10.1016/j.ijsolstr.2014.04.016.

[23] W. T. Koiter, "General theorems for elastic–plastic solids," in *Progress in Solids Mechanics*, I. N. Sneddon and R. Hill, Eds. Amsterdam , Netherlands: North-Holland Publishing Company, 1960.

[24] C. V. Le, P. H. Nguyen, and T. Q. Chu, "A curvature smoothing Hsieh–Clough–Tocher element for yield design of reinforced concrete slabs," *Computers & Structures*, vol. 152, pp. 59–65, May 2015, https://doi.org/10.1016/j.compstruc.2015.02.009.

[25] K. D. Andersen, E. Christiansen, and M. L. Overton, "Computing Limit Loads by Minimizing a Sum of Norms," *SIAM Journal on Scientific Computing*, vol. 19, no. 3, pp. 1046–1062, Jan. 1998, https://doi.org/10.1137/S1064827594275303.

[26] J. Lubliner, *Plasticity Theory*. New York, NY, USA: Macmillan, 1990.